Exploring land surface temperature earthquake precursors: A focus on the Gujarat (India) earthquake of 2001

Matthew Blackett,[1,2] Martin J. Wooster,[1] and Bruce D. Malamud[1]

Received 27 May 2011; revised 13 June 2011; accepted 26 June 2011; published 5 August 2011.

[1] There are many reports of land surface temperature (LST) anomalies appearing prior to large earthquakes. A number of methods have been applied in hindcast mode to identify these anomalies, using infrared datasets collected from Earth-orbiting remote sensing satellites. Here we examine three such methods and apply them to six years (2001–2006) of MODIS LST data collected over the region of the 2001 Gujarat (India) earthquake, which previous studies have identified as a site exhibiting possible pre-seismic and post-seismic thermal anomalies. Methods 1 and 2 use an LST differencing technique, while Method 3, the Robust Satellite Technique (RST), has been developed specifically for the identification of thermal anomalies within spatio-temporal datasets. In relation to the Gujarat Earthquake, results from Methods 1 and 2 (LST differencing) indicate that changes previously reported to be potential precursory thermal 'anomalies' appear instead to occur within the range of normal thermal variability. Results obtained with Method 3 (RST) do appear to show significant 'anomalies' around the time of the earthquake, but we find these to be related to positive biases caused by the presence of MODIS LST data gaps, attributable to cloud cover and mosaicing of neighboring orbits of data. Currently, therefore, we find no convincing evidence of LST precursors to the 2001 Gujarat earthquake, and urge care in the use of approaches aimed at identifying such seismic thermal anomalies. **Citation:** Blackett, M., M. J. Wooster, and B. D. Malamud (2011), Exploring land surface temperature earthquake precursors: A focus on the Gujarat (India) earthquake of 2001, *Geophys. Res. Lett.*, *38*, L15303, doi:10.1029/2011GL048282.

1. Introduction

[2] There is a long, sometimes controversial, history of research relating to earthquake precursors. Among such studies, many relate to possible thermal anomalies seen prior to large seismic events [e.g., *Wang and Zhou*, 1984; *Gornyy et al.*, 1988; *Qiang et al.*, 1997; *Panda et al.*, 2007; *Pergola et al.*, 2010]. Here we further explore some approaches used previously to identify 'precursory thermal anomalies' within infrared (IR) imagery taken from Earth-orbiting satellites, in particular examining the methods' sensitivities to time series length and data gaps caused by incomplete records and/or variations in cloudiness. We focus here on the M_W = 7.7 Gujarat (India) earthquake of 26 January 2001 (epicenter 23.41°N and 70.23°E) which killed over 20,000 people and caused over US$ 10 billion of damage [*Mishra et al.*, 2005; National Earthquake Information Center, Preliminary earthquake report, 2004, available at http://neic.usgs.gov/neis/eq_depot/2001/eq_010126/, accessed May 2011]. This event has been subject to a number of hindcast studies claiming to have identified thermal precursory signals using various IR remote sensing datasets [*Ouzounov and Freund*, 2004; *Saraf and Choudhury*, 2005a; *Genzano et al.*, 2007].

2. Background

[3] Early reports of possible air temperature variations related to seismic activity are detailed by *Milne* [1886], but the first attempts at measuring potential precursory Land Surface Temperature (LST) phenomena did not appear until the 1980s when, for example, *Wang and Zhou* [1984] claimed to have identified soil temperature 'anomalies' prior to the 1976 Chinese Tangshan Earthquake. *Gornyy et al.* [1988] went on to detail the use of satellite thermal infrared (TIR) data in identifying similar phenomena in Central Asian earthquake zones, and many subsequent works have also used satellite TIR data [e.g., *Genzano et al.*, 2007, *Pergola et al.*, 2010]. Other studies report significant (4–10 K) pre-seismic thermal anomalies across wide regions, based on analysis of satellite-retrieved LST data derived from TIR observations [e.g., *Saraf and Choudhury*, 2005b; *Panda et al.*, 2007]. However, while informative in many ways, these studies often appear limited in the quantity of data used to discriminate 'thermal anomalies' from natural variability [e.g., *Ouzounov and Freund*, 2004]. Furthermore, while some studies use more advanced statistical techniques [e.g., *Genzano et al.*, 2007; *Panda et al.*, 2007; *Genzano et al.*, 2009; *Pergola et al.*, 2010], the sensitivity of these approaches to data gaps caused by cloud cover or other data coverage variations has not been fully assessed. Here we analyze six full years (2001–2006) of daily MODIS LST data for the Gujarat region of India. We explore the existence of LST 'anomalies' related to this event using this extended dataset, along with analytical techniques based on those applied in previous earthquake thermal precursor studies [e.g., *Ouzounov and Freund*, 2004; *Filizzola et al.*, 2004; *Genzano et al.*, 2007].

3. Dataset Description

[4] We used daily night-time LST data for the Gujarat region, 2001–2006, extracted from the 1 km spatial resolution gridded v.4 MOD11A1 LST product, which is itself derived from TIR observations made by the MODIS instrument operating on board the polar-orbiting Terra spacecraft (detailed by *Wan* [1999]) (hereafter, MOD11A1). During 2001–2006, besides the 26 January 2001 Gujarat

[1]Environmental Monitoring and Modelling Research Group, Department of Geography, King's College London, London, UK.
[2]Now at Environment, Hazards and Risk Applied Research Group, Coventry University, Coventry, UK.

0094-8276/11/2011GL048282

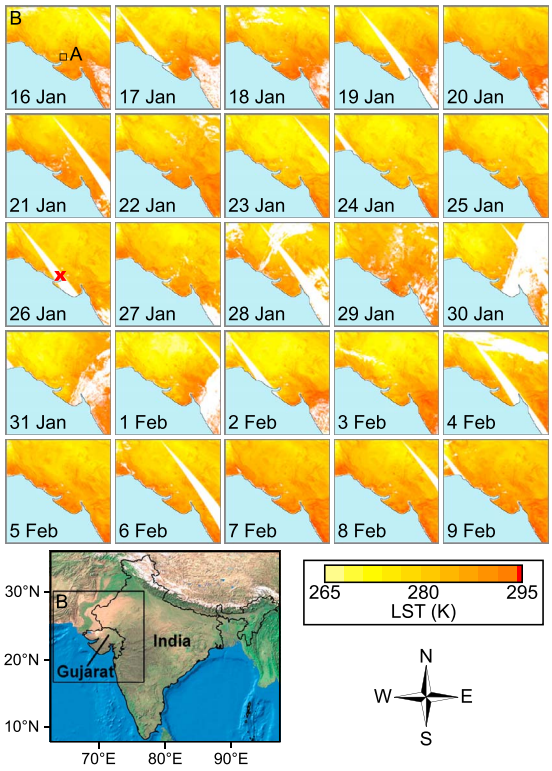

Figure 1. Night-time Land Surface Temperature (LST) maps for the Gujarat (India) region, 16 January–9 February 2001, with the 26 January 2001 Gujarat earthquake epicenter indicated by a red cross. Data are subset from the 1 km spatial resolution MODIS LST product (MOD11A1). This consists of data from the Terra MODIS sensor's night-time overpass (~22:15 to ~23:15 Indian Standard Time). LST data for two regions are presented, each centered on the earthquake epicenter (23.41°N, 70.23°E): (i) Region A: 100 km × 100 km, boxed area highlighted in the 16 January LST map; (ii) Region B: 1500 km × 1500 km (each LST map's total area). Region B is also boxed in the wider scale map at lower left (map source: ESRI, World Image.lyr, ArcGIS Software v. 10, Redlands, California, 1998). In each LST map, cloud cover and data gaps that remain between neighboring MODIS swaths are masked as white, while blue areas represent the Indian Ocean.

M_W = 7.7 earthquake, in a 750 km radius around Gujarat, there were no other similar-sized earthquakes (2nd largest earthquake, M_W = 5.8, 28 January 2001; two M_W = 5.5 in 2006 (National Earthquake Information Center, US Geological Survey earthquake database, 2011, available at http://earthquake.usgs.gov/earthquakes/eqarchives/epic/, accessed May 2011)).

[5] Two subsets of the Gujarat region were extracted for the six years of MOD11A1 data, both centered on the Gujarat earthquake epicenter: Region A (100 km × 100 km) formally examined by *Ouzounov and Freund* [2004], and a larger Region B (1500 km × 1500 km), representative of wider areas considered in other seismic thermal precursor studies [e.g., *Qiang et al.*, 1997; *Choudhury et al.*, 2006]. Example LST data from 25 days (16 January–9 February 2001) are shown in Figure 1 for Region B, with the smaller Region A shown boxed in the 16 January 2001 LST map. In these LST maps, light-blue represents the Indian Ocean (39.9% of 1500 × 1500 pixels in Region B).

[6] Each LST map (Figure 1) is derived from measurements of earth-emitted TIR spectral radiance made in MODIS bands 31 [11.00 μm] and 32 [12.02 μm], combined using the generalized split-window algorithm of *Wan and Dozier* [1996] and the land-cover classification-based emissivity approach of *Snyder et al.* [1998]. Cloudy pixels are masked using the methods of *Ackerman et al.* [2006]. To provide near complete spatial coverage on a daily basis, LST data derived from neighboring satellite orbits are mosaiced together in each MOD11A1 product file. Following this mosaicing process, areas with no useful LST data often remain in each product file due to cloud cover and gaps between the swaths of neighboring orbits, particularly at lower latitudes. In terms of accuracy, *Wolfe et al.* [2002] indicate that typical MODIS product geolocation precision is within 50 m (at nadir), and in a study focused on the Tibetan region, *Wang et al.* [2007] report that the MOD11A1 LST product displays a mean difference of 0.27 K when compared to *in situ* measures.

4. Methods

4.1. Data Processing

[7] Initial examining of the 1500 km × 1500 km Region B LST daily data, 2001–2006, found per-pixel LSTs as low as 197 K. Analysis of corresponding MODIS Level 1b radiance products confirmed these as cloudy pixels undetected by the *Ackerman et al.* [2006] tests. Using various LST minima thresholds, we remove these pixels, providing further 'cloud screening'. Unusable land pixels are white in Figure 1. After pre-processing the 2190 daily MOD11A1 scenes available 2001–2006, for Region A [B], 27% [17%] of scenes were classed unusable due to >75% of their land pixels having no usable LST data (cloud cover or mosaicing gaps); these scenes were removed from subsequent analysis. For Region A [B], the remaining 1601 [1820] scenes are used in our analyses, with 70% [89%] of the unusable scenes for Region A [B] occurring during the Indian Monsoon (June to September), and only 4% [1%] in the 5 January–16 February window (2001–2006) which in 2001 includes the Gujarat earthquake. All LST maps in Figure 1 (16 January–9 February 2001) are usable for Region B's study, and only the 26 January (Gujarat earthquake date) was removed for Region A.

[8] The final six-year, cloud-screened LST dataset had three methods applied to test for "pre-seismic" thermal anomalies:

[9] 1. Method 1 —LST difference between the 'earthquake' year and one other year, as used by *Ouzounov and Freund* [2004].

[10] 2. Method 2 — an extension of Method 1, based on the LST difference between each year of data (2001–2006) and the mean LST derived from all six years.

[11] 3. Method 3 — the Robust Satellite Technique (RST) statistical approach of *Tramutoli* [1998]. The RST was first developed for AVHRR thermal anomaly discrimination by *Tramutoli* [1998], and most recently applied to MODIS data of the 2009 L'Aquila (Italy) earthquake [*Pergola et al.*, 2010].

4.2. Method 1: LST Differencing (Based on Two Years)

[12] To test for potential thermal anomalies linked to the 2001 Gujarat earthquake, *Ouzounov and Freund* [2004] calculated the spatially averaged daily mean MODIS LST of an area equivalent to Region A (Figure 1) for a number of weeks either side of the earthquake, and for the equivalent days of the year in 2002. They then calculated the difference

between the 'earthquake' and 'non-earthquake' year measurements ($\Delta LST_{2001–2002}$) for each day of the year (DOY), and identified what they termed a "thermal anomaly pattern" [*Ouzounov and Freund*, 2004, p. 269]. We reproduce this method for Region A (5 January–16 February) and then extend the method to all other pairs of years $\Delta LST_{a\text{-}b}$, where a & b = (2001, 2002, …, 2006, $a \neq b$), i.e. up to 30 combinations per 'day'.

4.3. Method 2: Extended LST Differencing (Based on Multiple Years)

[13] Method 1 differences two years of data (a and b), so that the resulting measure ($\Delta LST_{a\text{-}b}$) is as much influenced by b (the 'baseline' year) as by a (the year of interest). To mitigate this influence, we repeat the approach of *Ouzounov and Freund* [2004] using Region A data, but extend it by deriving a 'climatological average' LST to which 2001 could be independently compared. We then applied the same procedure to all six years, calculating the spatially averaged mean LST for each DOY (d) for each *year* (2001, 20002, …, 2006), Region A, giving $LST\_A(d)_{year}$. Then, for a given DOY, up to six values are available (2001, 20002, …, 2006); these were averaged to provide 'climatological' mean DOY values ($\overline{LST\_A(d)}$) which were subtracted from the respective daily (d) values ($LST\_A(d)_{year}$). This quantifies the LST difference between the date of interest and the corresponding six-year mean ($\Delta LST_{A,year}$). We take $\Delta LST_{A,year}$ as our 'anomaly' measure, with up to 6 values for a given day of year.

4.4. Method 3: Robust Satellite Technique (RST)

[14] A detailed description of the RST as applied to remotely sensed LST data is given by *Filizzola et al.* [2004]. In summary, the technique functions by comparing the LST for a particular pixel and DOY (LST_r) to both the spatial mean of that particular scene ($LST\_A(d)_{year}$ and $LST\_B(d)_{year}$, Regions A and B respectively) and to the temporal mean (over multiple years considered) of LST for that particular pixel and DOY ($\overline{LST}_r$). This is normalized by the standard deviation (again, over multiple years) of the LST values for that particular pixel and DOY (σ [LST_r]). The aim is to provide a method of isolating pixels whose LST signal appears thermally anomalous when compared with the longer-term local spatial average [*Tramutoli*, 2007].

[15] Application of the RST results in the derivation of an index value (R_I) for each pixel (here given for Region A): $R_I = \{LST_r - LST\_A(d)_{year}) - \overline{LST}_r\}/\sigma$ [LST_r], where R_I represents the LST departure from the spatio-temporal historical 'average', weighted by its historical variability [*Genzano et al.*, 2009]. This index value is derived from the more general *Absolutely Local Index of Change of the Environment* (ALICE) of *Tramutoli* [1998]. When applied to seismic monitoring it is often referred to as the *Robust Estimator of TIR Anomalies* (RETIRA) [*Tramutoli et al.*, 2005; *Aliano et al.*, 2008a]. For a specific year, the RETIRA index value (R_I) for a given pixel and day can be interpreted as the number of standard deviations its LST (LST_r) is from that pixel's mean ($\overline{LST}_r$) for that DOY, over all years considered, adjusted for each scene's spatial mean.

[16] *Aliano et al.* [2008a] suggested that the RST can, in some cases, be impacted by the presence of cloud-related data 'gaps'. We explored and confirmed this using a set of LST simulations (see auxiliary material).[1] Despite potential bias in the RETIRA index caused by cloud-cover variations or other data gaps, use of the RST has continued in seismic thermal precursor studies [e.g., *Aliano et al.*, 2008b; *Genzano et al.*, 2009; *Pergola et al.*, 2010].

[17] We applied the RST to the six-year (2001–2006) MODIS LST dataset of Region A, so as to further examine the data at the scale used by *Ouzounov and Freund* [2004]. We then, as have other studies [e.g., *Qiang et al.*, 1997; *Choudhury et al.*, 2006; *Genzano et al.*, 2007], applied the RST to a much larger region (Region B). In these applications the six-year mean and standard deviation for each MOD11A1 pixel and DOY ($\overline{LST}_r$ and σ [LST_r], respectively), were calculated using a 15-day moving window of LST data, centered on the DOY in question. This ensured that even during persistent cloud cover or other data gaps, a significant number of observations (up to 15 per DOY for each of the six years, or 90 values) contributed to calculating $\overline{LST}_r$ and σ [LST_r] for each pixel.

[18] Here, we take the number of pixels (N_A and N_B) exceeding a selected R_I threshold in Regions A and B, respectively, as a measure of the degree to which the MOD11A1 data of a particular date contains LST 'anomalies'; N_A and N_B are expressed as a percentage of the total number of useable land pixels within the scene (*Percentage* N_A and *Percentage* N_B, respectively). In previous studies, R_I values have been classified as 'anomalous' using various thresholds, for example: >2.0, >2.5, >3.0 and >3.5 [*Tramutoli et al.*, 2005]; ≥2.0 and ≥3.0 [*Genzano et al.*, 2007]; and ≥2.0, ≥2.5 and ≥3 [*Pergola et al.*, 2010]. We found that over all DOY considered (2001–2006), the percentage of 'anomalous' pixels for different thresholds was for Region A [B]: $R_I \geq 2.0$ (2.27% [1.44%]), $R_I \geq 2.5$ (0.62% [0.29%]), and $R_I \geq 3.0$ (0.13% [0.06%]). We use $R_I \geq 2.5$ to represent 'anomalous' pixels.

5. Results

5.1. Method 1: LST Differencing (Based on Two Years)

[19] Figure 2a shows $\Delta LST_{a\text{-}b}$ derived using Method 1 as a function of DOY for Region A, 5 January–16 February, i.e. 26-days including the 26 January 2001 Gujarat earthquake date. The dotted line gives our reproduction of the *Ouzounov and Freund* [2004] $\Delta LST_{2001–2002}$ time series, where spatially averaged LST data from the same DOY in 2001 and 2002 are differenced. Extended to all six years (2001–2006), the envelopes are the maximum (pink) and minimum (blue) daily values for $\Delta LST_{a\text{-}b}$, with a & b = (2001, 2002, …, 2006). The dotted line ($\Delta LST_{2001–2002}$) shows a large local peak five days prior to the 26 January earthquake, as originally indicated by *Ouzounov and Freund* [2004], but compared against the backdrop of all the other years this peak no longer appears anomalous, with the upper envelope showing eight peaks of greater magnitude in this relatively short period of the year.

5.2. Method 2: Extended LST Differencing (Based on Multiple Years)

[20] Figure 2b shows the results of 'extended' LST differencing, where for each of the 26 days (5 January–

[1] Auxiliary materials are available in the HTML. doi:10.1029/2011GL048282.

16 February) we use six years of data (2001–2006) to calculate the mean LST to compare with each scene's LST (vs. just one year compared to another in Method 1). The dashed line shows our $\Delta LST_{A,2001}$ measure (section 4.2). Around the period of the 26 January earthquake, $\Delta LST_{A,2001}$ shows a similar pattern to that of the *Ouzounov and Freund* [2004] $\Delta LST_{2001–2002}$ time series (Figure 2a), both immediately prior to (and to some extent also subsequent to) the earthquake event itself.

[21] However, when we calculate $\Delta LST_{A,year}$, but this time substitute 2001, 2002, …, 2006, for the *year* being analyzed, as we found in Figure 2a, both comparable and larger peaks are actually seen in all other years (Figure 2b). The outer envelope of Figure 2b shows the maximum and minimum extent of $\Delta LST_{A,year}$ for each DOY (2001–2006), while Figure S1 in the auxiliary material shows the annually calculated measures used to construct this envelope. The envelope in Figure 2b indicates that the pre-event (and indeed post-event) LST peaks seen by *Ouzounov and Freund* [2004], and in our similar $\Delta LST_{A,2001}$ measure, although seemingly anomalous for this period in 2001, are not unusual when seen against $\Delta LST_{A,year}$ calculated for all six years. In particular, the $\Delta LST_{A,2001}$ peaks surrounding 26 January occur within the envelope of values found throughout the six-year period.

5.3. Method 3: Robust Satellite Technique (RST)

[22] Following the removal of scenes containing very significantly incomplete LST records in Region A [B] (see section 4.1), we now apply the RST (Method 3, described in section 4.3) to the remaining 1601 [1820] LST scenes for Region A [B]. We examine values of the RETIRA index, R_I, for each DOY. In applying the RST to our Region A [B] dataset, the number of scenes displaying 0 pixels with $R_I \geq 2.5$ was 42% [15%]. For each of the 1601 Region A LST scenes, after calculating R_I using all useable land pixels, the probability of a given value of R_I occurring was calculated.

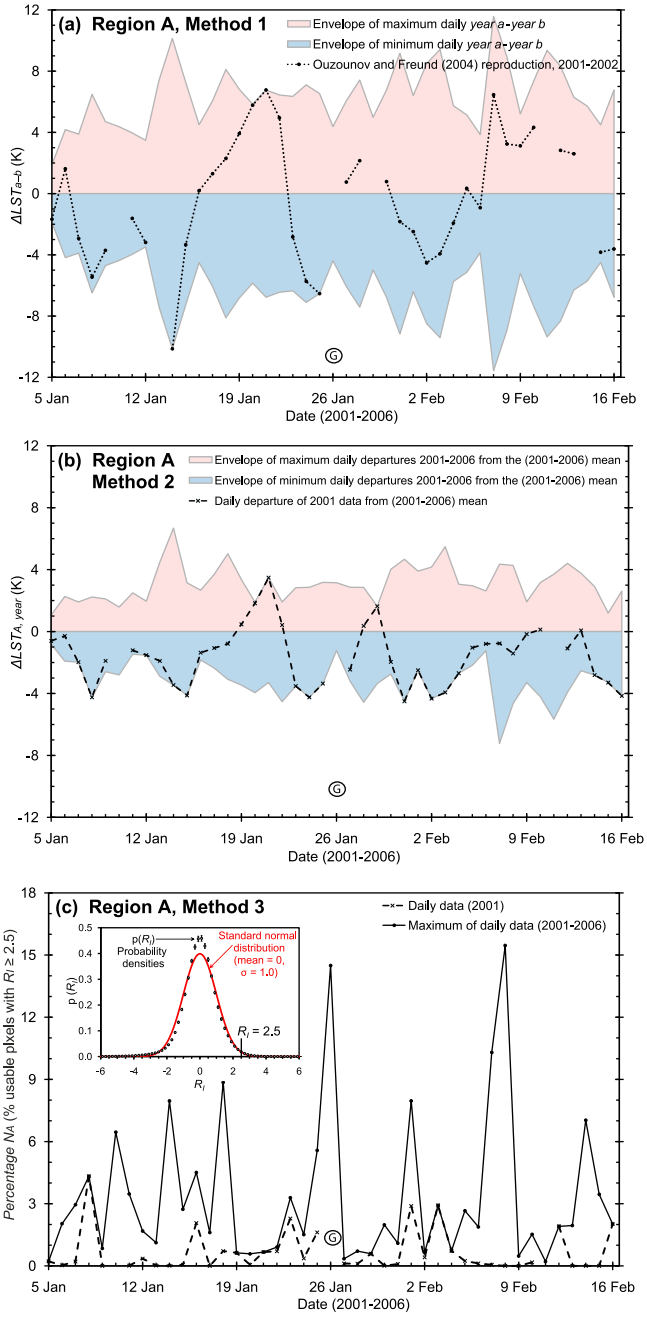

Figure 2. Land Surface Temperature (LST) differencing techniques, and Robust Satellite Technique (RST), applied to Region A (see Figure 1) for 5 January–16 February, 2001–2006. LST data were derived for each DOY (2001–2006) in the period surrounding the 26 January 2001 Gujarat earthquake, extracted from the 1 km spatial resolution MOD11A1 product for Region A (see Figure 1): (a) LST difference (two individual years) calculated as described in section 4.2 (Method 1) with the difference in Region A mean LST for a particular DOY (d) and *year* ($LST\_A(d)_{year}$) calculated between years a and b, ($\Delta LST_{a\text{-}b}$); a & b = (2001, 2002, …, 2006, $a \neq b$). The envelope of maximum (pink) and minimum (blue) daily values is shown for each DOY. The dotted black line ($\Delta LST_{2001–2002}$) is our reproduction of *Ouzounov and Freund* [2004] for the 'earthquake' year 2001 and the 'non-earthquake' 2002. (b) LST difference (multiple years) calculated as described in section 4.3 (Method 2). For a given day of year (d), the spatial average of LST for Region A in each of the six years was calculated ($LST\_A(d)_{year}$) and averaged to provide $\overline{LST\_A(d)}$. The dashed line is the daily departure from $\overline{LST\_A(d)}$ for the 2001 earthquake year, i.e. $\Delta LST_{A,2001} = LST\_A(d)_{2001} - \overline{LST\_A(d)}$. The colored envelope represents the daily maxima and minima of $\Delta LST_{A,year}$ calculated from data considering each of the six years (2001–2006) individually. (c) RETIRA index (R_I) values calculated using the RST [*Tramutoli*, 1998] as described in section 4.3 (Method 3). The dashed line shows the percentage of usable pixels with $R_I \geq 2.5$ (*Percentage* N_A) for 2001, while the solid line is the daily maxima of *Percentage* N_A for all six years, 5 January–16 February. The inset shows (circles with error bars) the average probability densities (±1 standard error) of R_I pixel values, for all 1601 usable scenes available over the six years, along with a standard normal distribution (red line, mean 0, standard deviation $\sigma = 1.0$). Thresholds of $R_I \geq 2.0$, 2.5 and 3.0 represent 2.27% (2σ), 0.62% (2.5σ), 0.13% (3σ), respectively, of the values in the probability density distribution. In Figures 2a–2c, breaks in the record are due to the removal of scenes with >75% of land pixels having no usable LST data. The Gujarat earthquake date (26 January 2001) is represented as a circled 'G'.

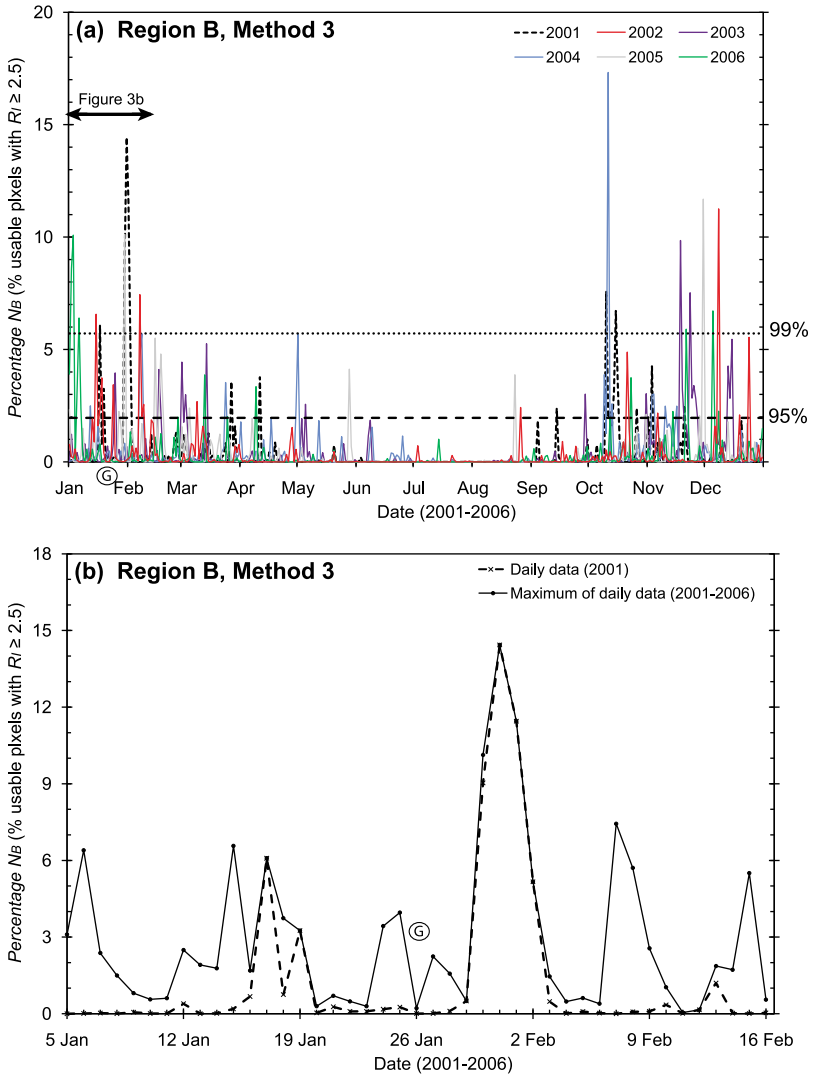

Figure 3. The Robust Satellite Technique (RST, Method 3) applied to daily MODIS LST data, 2001–2006, for a 1500 km × 1500 km area surrounding Gujarat, India. LST data were extracted from the 1 km spatial resolution v.4 MOD11A1 product for Region B (area covered by Figure 1 LST maps). Periods considered are (a) all days in the year, and (b) the six weeks (1 January–16 February) surrounding the date of the 26 January 2001 Gujarat earthquake. On the *y*-axis for Figures 3a and 3b is *Percentage* N_B, the percentage of usable pixels within the scene having RETIRA index [*Tramutoli et al.*, 2005] (see section 4.3) $R_I \geq 2.5$. The threshold of $R_I \geq 2.5$ represents the upper 0.29% of the probability density distribution of all R_I values for all usable scenes of the six year period (1820 scenes). The dashed black time series line for Figures 3a and 3b shows *Percentage* N_B for 2001, with each colored line in Figure 3a representing *Percentage* N_B for each of the six years, and the solid line in Figure 3b the daily maxima of *Percentage* N_B for all six years. In Figure 3a we use the 1820 scenes that remained following the removal of unusable scenes (i.e., those having data gaps covering >75% of land pixels). The horizontal dashed and dotted lines represent the 95th and 99th percentiles of *Percentage* N_B respectively. The Gujarat earthquake date (26 January 2001) is represented as a circled 'G'.

In Figure 2c (inset graph), p(R_I), the average probability density at a given R_I, is given over the range $-6 \leq R_I \leq 6$. The average probability densities of our 'real' data are reasonably similar to a standard Gaussian distribution (solid curve, Figure 2c, inset graph), i.e. mean 0, standard deviation 1.0.

[23] In Figure 2c we also present the *Percentage* N_A (percentage of useable land pixels with $R_I \geq 2.5$) in Region A as a function of DOY, 5 January–16 February. The dashed line shows the results for 2001 and the solid thin line the maximum of daily data for 2001–2006. The 2001 data (dashed line) shows a small peak (23 January) before the earthquake event in 2001, although offset slightly temporally in relation to the 'precursory LST peak' of Figure 2b. However, examination of maximum *Percentage* N_A data for all other years (solid line, Figure 2c) reveals many more peaks at other times, so we see no evidence for 'seismic thermal precursors' at the Region A scale.

[24] Figure 3a presents *Percentage* N_B (% of usable land pixels with $R_I \geq 2.5$) at the Region B scale, for every DOY (1–365), and year (2001–2006). It shows for 2001 (dashed line) large 'pre-seismic', and in particular 'post-seismic' peaks in *Percentage* N_B. Figure 3b focuses on 5 January–16 February, the 'earthquake period', and shows that for 2001, peaks around 17 and 19 January (pre-seismic) and

30 January–2 February (post-seismic), are the largest on those particular DOYs in the entire six years. Indeed, the post-seismic peak is the second-largest of the six-year period (Figure 2a), and both 'pre-' and 'post-seismic' peaks fall within the upper 1% of *Percentage* N_B values of all 1820 scenes for this dataset.

[25] Re-inspection of Figure 1 however, confirms that daily LST data coverage for Region B has varying degrees of completeness due to cloud cover and mosaicing gaps. For example, on the 16, 20, 30 January 2001, 11%, 3%, and 41% respectively of the land in Region B has no usable LST data. In particular, there are days (Figure 1) when substantial areas towards the south-east of Region B have no usable LST data (17–19 January and 30 January–2 February). With clear skies, the south-east exhibits the highest LSTs of the region, as confirmed when the spatial mean LST of the area covered by cloud on 30 January 2001 (283.5 K; standard deviation, σ = 1.5 K) is compared to that of the remaining cloud free surface for the period represented (281.7 K; σ = 1.8 K). The absence of data for this usually warmer region between 30 January and 2 February reduces the scene-wide LST mean ($LST\_B(d)_{year}$) for those dates, thereby lowering the LST required for any particular pixel to display $R_I \geq 2.5$ and producing the corresponding *Percentage* N_B peak (Figure 3b). The smaller, but still significant data gaps over this warmer south-east region around 17–19 January correspond with the smaller 'pre-cursory' *Percentage* N_B peak (Figure 3b). The magnitude of these peaks is subdued when higher R_I thresholds (i.e. $R_I \geq 3.0$ and $R_I \geq 3.5$) are applied, but so too is that of all other peaks, confirming that altering R_I thresholds fails to eliminate the bias caused by data gaps that mask normally warmer areas of the study region.

[26] The cause of these effects is a direct result of the mean LST of the scene being lowered due to some of the normally warmer area being unobserved and thus removed from the calculation, resulting in pixels with lower LSTs than would otherwise be the case appearing 'anomalous' based on R_I thresholding. The reverse happens when cloud masks a normally cooler region, and similarly there is little effect when cloud covers areas whose temperature is close to the scene average. Evidently cloud cover, and its precise location, can introduce significant bias into RST performance. We further explore and confirm this using simulations (Figures S2 and S3 in the auxiliary material).

6. Discussion and Conclusion

[27] The process of identifying potential thermal anomalies from within LST datasets requires the determination of 'baseline' conditions against which potential anomalies can be assessed. In general, the greater the number of years used to derive the measure of LST 'natural variability', the stronger can be the claim for any subsequent thermal anomaly identification. Here, for the 2001 Gujarat Earthquake, we have used up to six years of MODIS LST data to calculate the baseline from which LST departures are analyzed. We find that claims of seismic thermal precursors based on differencing only two years of data cannot be confirmed when we take into account the variability seen within a longer time series. Furthermore, we have shown that a more statistically-based method of thermal anomaly discrimination, the RST of *Tramutoli* [1998], can be significantly affected by positive biases when cloud cover or other data gaps affect normally warmer scene areas. We suppose that such effects could be responsible for at least some of the reports of seismic thermal precursors that have been noted, not just in the case of Gujarat [e.g., *Genzano et al.*, 2007], but also in other studies that have isolated these using the RST [e.g., *Tramutoli et al.*, 2005; *Pergola et al.*, 2010].

[28] In an attempt to potentially account for such effects when using the RST, *Genzano et al.* [2009] and *Pergola et al.* [2010] did remove remote sensing scenes displaying >80% cloud cover from their time series datasets. However, this would not have removed scenes such as that of 30 January 2001 examined here — which had no usable LST data for 41% of the Region B land surface pixels due to cloud-cover and swath-related data gaps — and which resulted in a significant peak in the percentage of pixels showing elevated RETIRA index values (Figure 3b). Evidently, if biases are to be avoided the precise location of cloud, in addition to its areal coverage, must be considered when the RST is applied. Based on our findings, we conclude that at present there is no robust evidence for the existence of LST anomalies prior to the 2001 Gujarat earthquake, and that reports of such precursory signals should be regarded cautiously until further instances of the phenomena become evident that stand up to detailed statistical scrutiny.

Notation

$LST\_A(d)_{year}$	spatial LST mean for a particular region (A), DOY (d) and year ($year$) (K).
$\overline{LST\_A(d)}$	mean $LST\_A(d)_{year}$ calculated using up to six years of data (K).
$\Delta LST_{A,year}$	the difference between $LST\_A(d)_{year}$ and $\overline{LST\_A(d)}$ (K).
$\Delta LST_{a\text{-}b}$	difference in mean LST for a particular DOY year between two years a and b.
LST_r	LST for a particular pixel and DOY (K).
$\overline{LST}_r$	mean LST for a particular pixel calculated using up to six years of data (K).
R_I	RETIRA index value (unitless).
N_A	number of pixels with $R_I > 2.5$ for a particular region (A).

[29] **Acknowledgments.** This work was supported by an SSPP PhD grant, King's College London. We thank NASA's Land Processes Distributed Active Archive Center (DAAC) for the data used in this study, and Stuart Gill (Coventry University) who assisted in cartography work.

References

Ackerman, S. A., K. I. Strabala, W. P. Menzel, R. A. Frey, C. C. Moeller, L. E. Gumley, B. A. Baum, S. Wetzel Seeman and H. Zhang (2006), Discriminating clear-sky from cloud with MODIS, Algorithm Theoretical Basis Document, ATBD MOD35, version 5.0, NASA Goddard Space Flight Cent., Greenbelt, Md.

Aliano, C., R. Corrado, C. Filizzola, N. Genzano, N. Pergola, and V. Tramutoli (2008a), Robust TIR satellite techniques for monitoring earthquake active regions: Limits, main achievements and perspectives, *Ann. Geophys.*, *51*, 303–318.

Aliano, C., R. Corrado, C. Filizzola, N. Pergola, and V. Tramutoli (2008b), Robust satellite techniques (RST) for the thermal monitoring of earthquake prone areas: The case of Umbria-Marche October, 1997 seismic events, *Ann. Geophys.*, *51*, 451–459.

Choudhury, S., S. Dasgupta, A. Saraf, and S. Panda (2006), Remote sensing observations of pre-earthquake thermal anomalies in Iran, *Int. J. Remote Sens.*, *27*, 4381–4396, doi:10.1080/01431160600851827.

Filizzola, C., N. Pergola, C. Pietraposa, and V. Tramutoli (2004), Robust satellite techniques for seismically active areas monitoring: A sensitivity

analysis on September 7, 1999 Athens's earthquake, *Phys. Chem. Earth*, *29*, 517–527.

Genzano, N., C. Aliano, C. Filizzola, N. Pergola, and V. Tramutoli (2007), A robust satellite technique for monitoring seismically active areas: The case of Bhuj–Gujarat earthquake, *Tectonophysics*, *431*, 197–210, doi:10.1016/j.tecto.2006.04.024.

Genzano, N., C. Aliano, R. Corrado, C. Filizzola, M. Lisi, G. Mazzeo, R. Paciello, N. Pergola, and V. Tramutoli (2009), RST analysis of MSG-SEVIRI TIR radiances at the time of the Abruzzo 6 April 2009 earthquake, *Nat. Hazards Earth Syst. Sci.*, *9*, 2073–2084, doi:10.5194/nhess-9-2073-2009.

Gornyy, V., A. G. Sal'man, A. A. Tronin, and B. V. Shilin (1988), Outgoing terrestrial infrared radiation as an indicator of seismic activity (in Russian), *Dokl. Akad. Nauk USSR*, *301*, 67–69.

Milne, J. (1886), *Earthquakes and Other Earth Movements*, D. Appleton, New York.

Mishra, D. C., C. V. Chandrasekhar, and B. Singh (2005), Tectonics and crustal structures related to Bhuj earthquake of January 26, 2001: Based on gravity and magnetic surveys constrained from seismic and seismological studies, *Tectonophysics*, *396*, 195–207, doi:10.1016/j.tecto.2004.12.007.

Ouzounov, D., and F. Freund (2004), Mid-infrared emission prior to strong earthquakes analyzed by remote sensing data, *Adv. Space Res.*, *33*, 268–273, doi:10.1016/S0273-1177(03)00486-1.

Panda, S. K., S. Choudhury, A. K. Saraf, and J. D. Das (2007), MODIS land surface temperature data detects thermal anomaly preceding 8 October 2005 Kashmir earthquake, *Int. J. Remote Sens.*, *28*, 4587–4596, doi:10.1080/01431160701244906.

Pergola, N., C. Aliano, I. Coviello, C. Filizzola, N. Genzano, T. Lacava, M. Lisi, G. Mazzeo, and V. Tramutoli (2010), Using RST approach and EOS-MODIS radiances for monitoring seismically active regions: A study on the 6 April 2009 Abruzzo earthquake, *Hazards Earth Syst. Sci.*, *10*, 239–249, doi:10.5194/nhess-10-239-2010.

Qiang, Z., X. Xu, and C. Dian (1997), Case 27: Thermal infrared anomaly precursor of impending earthquakes, *Pure Appl. Geophys.*, *149*, 159–171, doi:10.1007/BF00945166.

Saraf, A. K., and S. Choudhury (2005a), NOAA-AVHRR detects thermal anomaly associated with the 26 January, 2001 Bhuj earthquake, Gujarat, India, *Int. J. Remote Sens.*, *26*, 1065–1073, doi:10.1080/01431160310001642368.

Saraf, A. K., and S. Choudhury (2005b), Satellite detects surface thermal anomalies associated with the Algerian earthquakes of May 2003, *Int. J. Remote Sens.*, *26*, 2705–2713, doi:10.1080/01431160310001642359.

Snyder, W., Z. Wan, Y. Zhang, and Z. Feng (1998), Classification-based emissivity for land surface temperature measurement from space, *Int. J. Remote Sens.*, *19*, 2753–2774, doi:10.1080/014311698214497.

Tramutoli, V. (1998), Robust AVHRR techniques (RAT) for environmental monitoring: Theory and applications, in *Earth Surface Remote Sensing II*, edited by G. Cecchi and E. Zilioli, *Proc. SPIE*, 3496, 101–113.

Tramutoli, V. (2007), Robust satellite techniques (RST) for natural and environmental hazards monitoring and mitigation: Theory and applications, in *Proceedings of Multi Temp 2007*, pp. 1–6, Inst. of Electr. and Electron. Eng., New York, doi:10.1109/MULTITEMP.2007.4293057.

Tramutoli, V., V. Cuomo, B. Filizzola, N. Pergola, and C. Piertraposa (2005), Assessing the potential of thermal infrared satellite surveys for monitoring seismically active areas: The case of Kocaeli (Izmit) earthquake, August 17, 1999, *Remote Sens. Environ.*, *96*, 409–426, doi:10.1016/j.rse.2005.04.006.

Wan, Z. (1999), MODIS land surface temperature, Algorithm Theoretical Basis Document (LST ATBD), version 3.3, NASA Goddard Space Flight Cent., Greenbelt, Md.

Wan, Z., and J. Dozier (1996), A generalized split-window algorithm for retrieving land surface temperature from space, *IEEE Trans. Geosci. Remote Sens.*, *34*, 892–905.

Wang, K., Z. Wan, P. Wang, M. Sparrow, J. Liu, and S. Haginoya (2007), Evaluation and improvement of the MODIS land surface temperature/emissivity products using ground-based measurements at a semi-desert site on the western Tibetan Plateau, *Int. J. Remote Sens.*, *28*, 2549–2565, doi:10.1080/01431160600702665.

Wang, L., and C. Zhou (1984), Anomalous variations of ground temperature before the Tangsan and Haiheng earthquakes (in Chinese), *J. Seismol. Res.*, *7*, 649–656.

Wolfe, R., M. Nishihama, A. Fleig, J. Kuyper, D. Roy, C. Storey, and F. Patt (2002), Achieving sub-pixel geolocation accuracy in support of MODIS land science, *Remote Sens. Environ.*, *83*, 31–49, doi:10.1016/S0034-4257(02)00085-8.

M. Blackett, Environment, Hazards and Risk Applied Research Group, Coventry University, Coventry CV1 5FB, UK. (matthew.blackett@coventry.ac.uk)

B. D. Malamud and M. J. Wooster, Environmental Monitoring and Modelling Research Group, Department of Geography, King's College London, London WC2R 2LS, UK.